Toward self-tuning adaptive vibration based micro-generators

Shad Roundy and Yang Zhang
Australian National University, Dept. of Engineering, Canberra, ACT 0200, Australia

ABSTRACT

The rapidly decreasing size, cost, and power consumption of wireless sensors has opened up the relatively new research field of energy harvesting. Recent years have seen an increasing amount of research on using ambient vibrations as a power source. An important feature of all of these generators is that they depend on the resonance frequency of the generator device being matched with the frequency of the input vibrations. The goal of this paper, therefore, is to explore solutions to the problem of self-tuning vibration based energy harvesters. A distinction is made between "active" tuning actuators that must continuously supply power to achieve the resonance frequency change, and "passive" tuning actuators that supply power initially to tune the frequency, and then are able to "turn off" while maintaining the new resonance frequency. This paper analyzes the feasibility of tuning the resonance frequency of vibration based generators with "active" tuning actuators. Actuators that can tune the effective stiffness, mass, and damping are analyzed theoretically. Numerical results based for each type of actuator are presented. It is shown that only actuators that tune the effective damping will result in a net increase in power output, and only under the circumstance that no actuation power is needed to add damping. The net increase in power occurs when the mismatch between driving vibrations the mismatch between driving vibrations the resonance frequency of the device is more than 5%. Finally, the theory and numerical results are validated by experiments done on a piezoelectric generator with a smart material "active" tuning actuator.

Keywords: energy scavenging, vibration, self-tuning, piezoelectric

1. INTRODUCTION

Recent years have seen a dramatic increase in energy harvesting research applied to wireless sensors. This research interest has been driven largely by the vast reduction in power and size of the CMOS circuitry associated with wireless sensor devices. For example, the power requirements for wireless sensor devices has been reduced to well below 1 mW[1], opening up the possibility of completely powering the device from energy scavenged from the environment.

A significant amount of research has been published on vibration based generators that make use of the piezoelectric effect[2-4], electromagnetic coupling[5-7], or electrostatic coupling[8-10]. An important feature of all of these generators is that they depend on the resonance frequency of the generator device being matched with the frequency of the input vibrations. The generators tend to have fairly low damping ratios resulting in quality factors around 20 [4]. Therefore, if there is a significant mismatch between input and resonance frequencies, the power output drops very quickly to levels too low to be of use by wireless sensors. While it is feasible in many applications to design a generator device for a specific vibration environment that will not change (e.g. HVAC ducts), the frequency of the driving vibrations depends on the operating conditions in many other environments (e.g. an automobile). Therefore, it would be highly desirable if the generator could tune its own resonance frequency, in real-time, to match that of the driving vibrations. Whether or not this can be done in such a way as to increase the net power output is still an open question.

The frequency tuning could be done by "active" actuators in which the change in frequency is accomplished by an actuator that is "on" at all times. An example of this type of tuning actuator would be electrostatic springs[11]. This approach will be referred to as "active tuning". The frequency tuning could also be accomplished by an actuator that turns "on" to tune the generator, and then is able to turn "off" while maintaining the new resonance frequency. Examples include a moveable clamp which would change the length (and stiffness) of a flexure mechanism, a moveable mass, or flexures that could be tensioned and re-clamped. This approach will be referred to as "passive tuning".

Smart Structures, Devices, and Systems II, edited by Said F. Al-Sarawi,
Proceedings of SPIE Vol. 5649 (SPIE, Bellingham, WA, 2005)
0277-786X/05/$15 · doi: 10.1117/12.581887

While the passive tuning approach also needs to be evaluated, the purpose of this paper is to analyze the feasibility of tuning the resonance frequency of vibration based generators with active tuning actuators. A general theory regarding the tuning of generators will be presented along with numerical results based on this theory. Finally, a piezoelectric generator with a tuning actuator has been developed, and test results from this generator will be presented.

2. BASIC THEORY

The general theory developed in this section will provide expressions for the power required to tune the resonance frequency and compare that power to the theoretical electrical power output. The goal is to analytically determine the extent to which the resonance frequency can be altered while still maintaining a net positive power output, and whether this net power output is greater than would be obtained without the use of a tuning actuator.

2.1. General power conversion model

The theory presented in this section is based on the linear vibration based generator model presented by Williams and Yates[5]. The primary idea behind this model is that the generator behaves like a second order mechanical system. The electrical energy removed from the oscillating mechanical system behaves like viscous damping from the point of view of the mechanical system. Figure 1 shows a schematic of the system where b_m represents mechanical viscous damping (or pure loss) and b_e represents the damping introduced by the electrical load. Note that a tuning actuator force $F_a(t)$ is also shown on the schematic, but is only used to derive the power expressions for tuning, which are presented later.

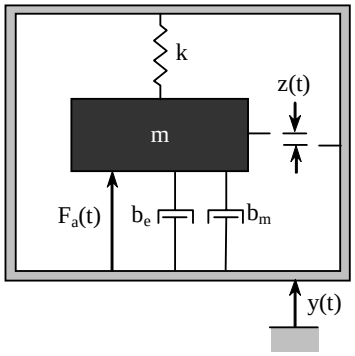

Figure 1. Schematic of generic vibration based generator.

Neglecting the tuning actuator, the dynamics of the system are given by:

$$m\ddot{z} + (b_e + b_m)\dot{z} + kz = -m\ddot{y} \tag{1}$$

where y represents the input vibrations, z is the displacement of the mass with respect to the generator frame (e.g. the deflection of the spring), m is the proof mass, k is the stiffness, b_m is the mechanical damping coefficient, and b_e is the electrically induced damping coefficient.

The power transferred to the electrical load is equal to the power removed from the mechanical system by damper b_e. Therefore, the output electrical power is given by:

$$P = \frac{1}{2} b_e \dot{z}^2 \tag{2}$$

Assuming a sinusoidal excitation, equations 1 and 2 can be used to derive the following frequency domain expression for the output electrical power:

$$\left|P_{out}\right| = \frac{m\zeta_e\left(\frac{\omega}{\omega_n}\right)^3 A^2}{\omega\left[\left(2\zeta\frac{\omega}{\omega_n}\right)^2 + \left(1-\left(\frac{\omega}{\omega_n}\right)^2\right)^2\right]} \tag{3}$$

where ω is the frequency of the input vibrations, ω_n is the resonance frequency of the generator, ζ_e is the electrically induced damping ratio ($\zeta_e = 2mb_e\omega_n$), ζ is the composite damping ratio ($\zeta_e + \zeta_m$), and A is the acceleration magnitude of the input vibrations.

In the case where the resonance frequency matches the driving frequency ($\omega_n = \omega$), the output power can be further reduced to the following expression:

$$\left|P_{out}\right| = \frac{m\zeta_e A^2}{4\omega\zeta^2} \tag{4}$$

The Williams model characterizes an electromagnetic generator quite well. Piezoelectric and electrostatic generators are not represented as well by this model. However, the model does characterize important aspects of piezoelectric and electrostatic systems. Specifically, the power output is proportional to mass, inversely proportional to frequency (at constant input acceleration magnitude), and inversely proportional to the mechanical damping. Furthermore, there is an optimal level of electrically induced damping (or apparent electrical load impedance). Finally, the model does give a reasonable estimate of theoretical power output for any type of generator[4]. Therefore, the Williams model seems an appropriate model to evaluate the attractiveness of frequency tuning techniques.

The power will be maximum when the system is oscillating at its natural frequency, which is simply given by:

$$\omega_n = \sqrt{k/m} \tag{5}$$

Therefore, in order to tune the generator, an actuator must alter the effective stiffness or mass. Or, in other words, the natural frequency can be altered by providing an additional force proportional to the generator's displacement (i.e. alter stiffness), or acceleration (i.e. alter mass). A second consideration is that by altering the damping, the bandwidth of the system could be increased at the expense of the quality factor. Under certain circumstances this could improve the net power output. So, a third option is to provide a force proportional to the velocity (i.e. alter the damping).

2.2. Effective stiffness and mass tuning actuators

First, consider the case in which the tuning actuator alters the effective stiffness (or provides a force proportional to the displacement). Then $F_a(t) = k_a z(t)$. The power ($P_a(t)$) required by this actuator is:

$$P_a(t) = k_a z(t)\dot{z}(t) \tag{6}$$

Assume that the actuator alters the system resonance from the original natural frequency (ω_1) to a new natural frequency (ω_2). Then ω_2 is given by:

$$\omega_2 = \sqrt{\frac{k + k_a}{m}} \tag{7}$$

The actuator stiffness, k_a, can then be represented as:

$$k_a = m\omega_2^2 - k = m\left(\omega_2^2 - \omega_1^2\right) \tag{8}$$

The displacement of proof mass can be expressed as $z(t) = Z\sin(\omega_2 t)$, and the velocity as $\dot{z}(t) = \omega_2 Z\cos(\omega_2 t)$, where Z is the magnitude of $z(t)$. Substituting these two expressions, and equation 8 into equation 6 yields

$$P_a(t) = m\omega_2\left(\omega_2^2 - \omega_1^2\right)Z^2 \sin(\omega_2 t)\cos(\omega_2 t) \tag{9}$$

Equation 9 can be rewritten as in 10.

$$P_a(t) = \frac{1}{2}m\omega_2\left(\omega_2^2 - \omega_1^2\right)Z^2 \sin(2\omega_2 t) \tag{10}$$

Assuming that the frequency of the input vibrations is at ω_2, Z can be expressed as:

$$Z = \frac{A}{2\zeta\omega_2^2} \tag{11}$$

Substituting equation 11 into 10, the magnitude of the actuation power becomes:

$$\left|P_a\right| = \frac{m\left(\omega_2^2 - \omega_1^2\right)A^2}{8\zeta^2\omega_2^3} \tag{12}$$

Let r be the ratio of tuned natural frequency to original natural frequency ($r = \omega_2/\omega_1$). Equation 12 can then be rewritten as:

$$\left|P_a\right| = \frac{m\left(r^2 - 1\right)A^2}{8\zeta^2 r^3\omega_1} \tag{13}$$

Next, consider the case in which the tuning actuator alters the effective mass (or provides a force proportional to the acceleration). Then $F_a(t) = m_a\,\dot{z}(t)\ddot{z}(t)$. The power ($P_a(t)$) required by this actuator is:

$$P_a(t) = m_a\dot{z}(t)\ddot{z}(t) \tag{14}$$

Following the same procedure as presented above in equations 7 through 13, the resulting expression for the magnitude of the actuation power is identical to that in equation 13.

2.3. Power output for effective stiffness and mass tuning actuators

With the expressions in equations 3, 4 and 13 established, we are now in a position to determine the condition under which tuning the natural frequency of the generator can result in a net increase in electrical power output. Assume, as before, that the frequency of the driving vibrations is ω_2 and the un-tuned natural frequency of the generator is ω_1. Then, there will be a net increase in power output only if the following inequality is true.

$$\left|P_{out2}(\omega_2)\right| - \left|P_a\right| \geq \left|P_{out1}(\omega_2)\right| \tag{15}$$

where $P_{out2}(\omega_2)$ is the power output after tuning, P_a is the actuation power, and $P_{out1}(\omega_2)$ is the power output without tuning at an input frequency of ω_2.

The power output after tuning ($P_{out2}(\omega_2)$) is simply given by equation 4 where $\omega = \omega_2$. The actuation power (P_a) is given by equation 13. An expression for the power output without tuning ($P_{out1}(\omega_2)$) is obtained by substituting $\omega = \omega_2$ and $\omega_n = \omega_1$ into equation 3. With the further substitution of $r = \omega_2/\omega_1$, the expression for $P_{out1}(\omega_2)$ is:

$$\left|P_{out1}(\omega_2)\right| = \frac{m\zeta_e r^2 A^2}{4\zeta^2 r^2\omega_1 + \omega_1\left(1 - r^2\right)^2} \tag{16}$$

It is important to note that the following limits on variables will always be true: $r > 0$, $\zeta > 0$, $\zeta_e > 0$, $\zeta > \zeta_e$. Therefore, $P_{out2}(\omega_2)$ and $P_{out1}(\omega_2)$ are always positive. Substituting equations 4, 13, and 16 into equation 15, and rearranging algebraically yields the following inequality:

$$-\left|r^2-1\right| \geq \left(r^2-1\right)\frac{2r\zeta_e\left(4r^2\zeta^2+\left(1-r^2\right)\right)}{4r^2\zeta^2+\left(1-r^2\right)^2} \tag{17}$$

Two situations of interest exist: $r > 1$ and $r < 1$. Note that $r = 1$ is not of interest since that means that the driving frequency exactly matches the untuned natural frequency. These two situations will be considered separately. If $r > 1$, then $|r^2-1| = r^2 - 1$. Using this fact, and the fact that $\zeta_e < \zeta$, the inequality in 17 can be reduced to:

$$\left(\left(1-r^2\right)+2r\zeta_e\right)^2 \leq 0 \tag{18}$$

which is never true for any value of r or ζ_e.

Next, consider the situation in which $0 < r < 1$. Then $|r^2-1| = -(r^2 - 1)$. Again, using this fact, and the fact that $\zeta_e < \zeta$, the inequality in 17 can be reduced to:

$$-\left(\left(1-r^2\right)+2r\zeta\right)^2 \geq 0 \tag{19}$$

which is never true for any value of r or ζ.

Therefore, an "active" actuator that tunes the natural frequency of the generator by altering either the effective stiffness or mass will never result in a net increase in electrical power output as long as the system is well represented by the Williams model.

2.4. Numerical results from effective stiffness and mass tuning generators

Figure 2 gives a visual illustration of the theory presented above. The three power elements of inequality 15 above are shown in the figure versus the ratio of tuned natural frequency to untuned natural frequency ($r = \omega_2/\omega_1$). Additionally, the net change in power output from tuning ($|P_{out2}|-|P_a|-|P_{out1}|$) is shown. As per inequality 15 above, the net change in power output should be positive if the frequency tuning is to have a beneficial effect. As the theory predicts, the net power change is not positive for any value of r. The simulation shown in Figure 2 was performed with a mass of 10 grams, untuned natural frequency of 100 Hz, and damping ratio of 0.03. However, the results are the same for any positive mass, natural frequency, and damping ratio.

2.5. Altering the damping ratio

Next consider the case in which an actuator alters the damping characteristics of the generator. From equation 1, $|Z(j\omega)|$ can expressed as:

$$\left|Z(j\omega)\right| = \frac{A/\omega_n^2}{\sqrt{4\zeta^2\left(\frac{\omega}{\omega_n}\right)^2+\left(1-\left(\frac{\omega}{\omega_n}\right)^2\right)^2}} \tag{20}$$

Taking the derivative of equation 20 with respect to ω, setting it equal to zero, and solving for ω yields the value of ω for which $|Z(j\omega)|$ is optimized. The optimal value of ω is the damped natural frequency (or ω_d).

However, the magnitude of the power output ($|P(j\omega)|$) is maximized for $\omega = \omega_n$, not $\omega = \omega_d$. The expression for $|P(j\omega)|$ is given above as equation 3. Using the same procedure to find the frequency at which $|P(j\omega)|$ is optimized yields $\omega = \omega_n$. This is illustrated below in Figure 3, which shows both the output displacement and power versus frequency for damping ratios ranging from 0.01 to 0.2. Note from the figure that while the displacement is greatest for $\omega = \omega_d$, which is a function of the damping ratio, the power is greatest for $\omega = \omega_n$, which is independent of the damping ratio. This can be explained by the fact that the power is proportional to the output velocity ($\dot{z}$), not the displacement, and $|\dot{Z}(j\omega)| = \omega|Z(j\omega)|$.

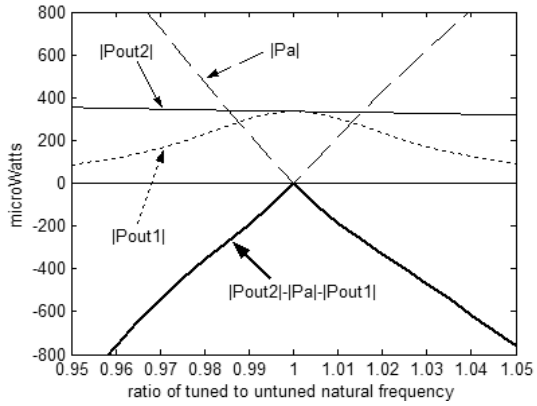

Figure 2. Power output after tuning ($|P_{out2}|$), power output without tuning ($|P_{out1}|$), tuning actuation power ($|P_a|$) and net output power change from tuning ($|P_{out2}|-|P_a|-|P_{out1}|$) versus ratio of tuned natural frequency to original natural frequency ($r = \omega_2/\omega_1$).

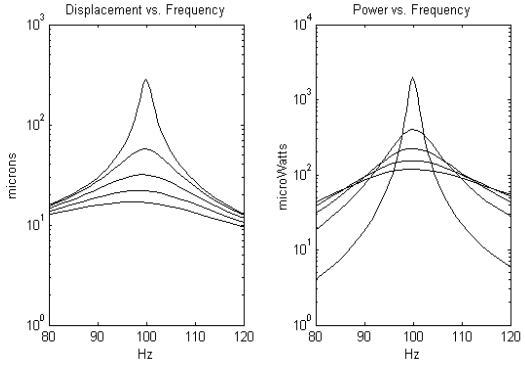

Figure 3. Displacement and power output versus frequency for damping ratios ranging from 0.01 to 0.2. The optimal frequency for displacement decreases with increasing damping, while the optimal frequency for power is independent of the damping ratio.

Therefore, altering the damping characteristics will not alter the frequency at which the power output is maximized. So, assuming that the Williams model is a valid power conversion model, if the input frequency does not matched the *undamped* natural frequency, trying to tune the resonance frequency of the system by altering damping will not result in increased power output.

It will be noticed from Figure 3 however, that if the driving frequency does not match the undamped natural frequency very closely, a lower Q system (one with more damping) will result in a higher power output. Therefore, although not altering the peak frequency of the power spectrum, increasing the damping could improve the power output if the driving and resonance frequencies do not match. It is natural to assume that the "extra" damping in this situation would be electrically induced damping. First, in most cases, it will be easier to control the electrically induced damping. Second, the net power output will naturally be higher by increasing the electrically induced damping as opposed to increasing the mechanical damping which represents pure loss.

Assume that an actuator (which may be purely electronic) that can control the electrically induced damping (ζ_e) is applied to the system. Further assume that without the actuator, the electrically induced damping ratio (ζ_e) is equal to the mechanical damping ratio (ζ_m), its optimal value. Assuming that this is an "active" actuator, as described above, the magnitude of the power consumed by this actuator is

$$\left|P_a(j\omega)\right| = \frac{m\zeta_{ea}\left(\frac{\omega}{\omega_n}\right)^3 A^2}{\omega\left\{\left[2(2\zeta_m+\zeta_{ea})\frac{\omega}{\omega_n}\right]^2+\left[1-\left(\frac{\omega}{\omega_n}\right)^2\right]^2\right\}} \tag{21}$$

where ζ_{ea} represents the extra damping provided by the actuator. Let P_{out1} be the output power without the actuator (i.e. any "extra" damping). Then the magnitude of P_{out1} is given by

$$\left|P_{out1}(j\omega)\right| = \frac{m\zeta_m\left(\frac{\omega}{\omega_n}\right)^3 A^2}{\omega\left\{\left[4\zeta_m\frac{\omega}{\omega_n}\right]^2+\left[1-\left(\frac{\omega}{\omega_n}\right)^2\right]^2\right\}} \tag{22}$$

Let P_{out2} be the output power after the extra damping is applied. P_{out2} is then give by

$$|P_{out2}(j\omega)| = \frac{m(\zeta_m + \zeta_{ea})\left(\frac{\omega}{\omega_n}\right)^3 A^2}{\omega\left\{\left[2(2\zeta_m + \zeta_{ea})\frac{\omega}{\omega_n}\right]^2 + \left[1-\left(\frac{\omega}{\omega_n}\right)^2\right]^2\right\}} \tag{23}$$

As before, the net change in power output is $|P_{net}| = |P_{out2}| - |P_a| - |P_{out1}|$. Equation 24 gives an analytical expression for $|P_{net}|$.

$$|P_{net}| = \frac{-4m\omega_n^3\omega^4\zeta_m\zeta_{ea}(4\zeta_m + \zeta_{ea})A^2}{\left[4\omega_n^2\omega^2(2\zeta_m + \zeta_{ea})^2 + (\omega_n^2 - \omega^2)^2\right]\left[16\omega_n^2\omega^2\zeta_m^2 + (\omega_n^2 - \omega^2)^2\right]} \tag{24}$$

From equation 24, $|P_{net}|$ must clearly always be negative for positive values of ω, ω_n, ζ_m, and ζ_{ea}. Therefore, as with "active" stiffness and mass actuators, an "active" damping actuator will never result in improved power output. This is illustrated visually for one set of parameters in Figure 4.

In reality, adjusting the electrically induced damping ratio by adjusting the characteristics of the electrical load would probably not require a constant power input. Thus, it is unlikely that such a system would constitute an "active" actuator. If the trivial, but possibly not too far off, assumption is made that adjusting the damping ratio requires no power (i.e. $|P_a| = 0$), then $|P_{net}| = |P_{out2}| - |P_{out1}|$. An analytical expression for $|P_{net}|$ in this case is given in equation 25.

$$|P_{net}| = \frac{-m\omega_n\omega^2\zeta_{ea}\left((\omega_n^2 - \omega^2)^2 - 4\omega^2\omega_n^2\zeta_m\zeta_{ea}\right)}{\left[4\omega_n^2\omega^2(2\zeta_m + \zeta_{ea})^2 + (\omega_n^2 - \omega^2)^2\right]\left[16\omega_n^2\omega^2\zeta_m^2 + (\omega_n^2 - \omega^2)^2\right]} \tag{25}$$

In contrast to the expression in equation 24, the value of P_{net} as expressed in equation 25 can be positive or negative depending on the values of ζ_m, ζ_{ea}, ω, and ω_n. A graphical example is shown Figure 5 using the same set of parameters as the example shown in Figure 4.

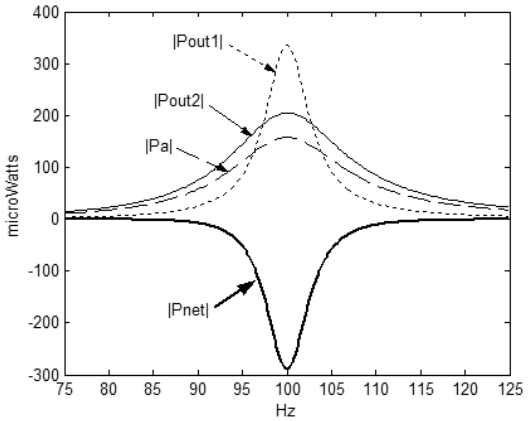

Figure 4. Power output with no extra damping ($|P_{out1}|$), after extra damping is applied ($|P_{out2}|$), from damping actuator ($|P_a|$) and net change in power output ($|P_{net}|$) vs. frequency. ζ_m = 0.015, $\zeta_e = \zeta_m$, and ζ_{ea} = 0.05 for this example.

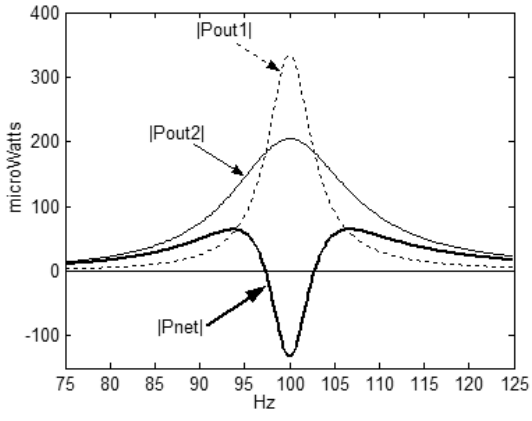

Figure 5. Power output with no extra damping ($|P_{out1}|$), after extra damping is applied ($|P_{out2}|$), and net power out ($|P_{net}|$) vs. frequency. It is assumed that $|P_a| = 0$, ζ_m = 0.015, $\zeta_e = \zeta_m$, and ζ_{ea} = 0.05 for this example.

In the example shown in Figure 5, the power output can be improved by increasing the electrically induced damping if the driving frequency does not match the resonance frequency. In this example, if the driving and resonance frequencies matched, the output power would be 335 μW. However if the input frequency were at either 93 Hz or 107

Hz (the optimal points for the P_{net} curve), the power output without extra damping ($|P_{out1}|$) is 60 μW, the power output with extra damping ($|P_{out2}|$) is 124 μW. Therefore the net power improvement from altering the damping is 64 μW. However, the power output is still less than half of what it would be if the resonance frequency matched the driving frequency. It is also important to note that this situation does not constitute an "active" tuning actuator as the system can maintain its tuned natural frequency with no actuation power.

Thus, regardless of the phase of the actuation force, the increased power output will always be more than offset by the required actuation force. This conclusion is valid as long as the system can be reasonably well modeled by the Williams model.

3. DESIGN AND MODELING OF A TUNABLE PIEZOELECTRIC BENDING GENERATOR

Piezoelectric benders mounted as cantilever beams have been used as vibration based generators[2-4]. Such generators can be actively tuned by creating two electrodes on the surface of the beam, one for scavenging and the other for tuning. A schematic of this type of device is shown in Figure 6. The apparent stiffness of a piezoelectric material is dependent on both the elastic constant of the material, and the electric field across the material. Thus, by controlling the voltage across the tuning electrode, the natural frequency of the system can be controlled. In particular, driving the tuning electrode with a signal that is 180 degrees out of phase with the signal from the scavenging electrode will "soften" the beam and reduce its apparent stiffness.

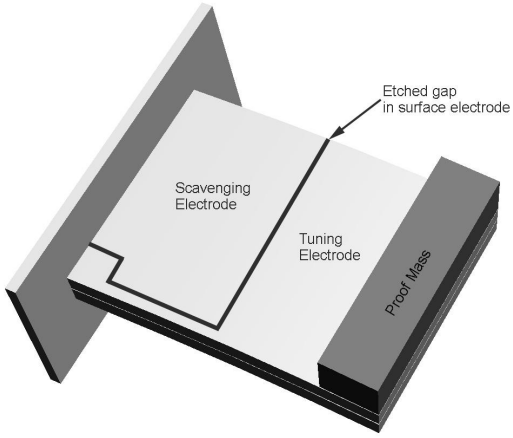

Figure 6. Schematic of a piezoelectric bender mounted as a cantilever beam. The surface electrode is etched to create a scavenging and a tuning electrode.

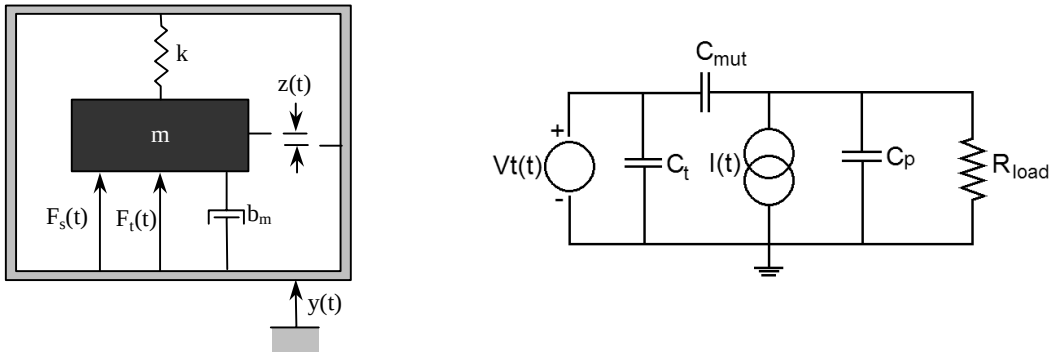

Figure 7. Mechanical and circuit schematic of piezoelectric generator with tuning electrode. $F_s(t)$ is the force resulting from the coupling of the material under the scavenging electrode, and $F_t(t)$ is the force from the coupling of the material under the tuning electrode.

The system can be modeled as a simple spring mass system and circuit as demonstrated by the schematic in Figure 7. The two forces result from the voltage across the scavenging and tuning electrodes. The current source represents the current scavenged from the scavenging electrode. C_p is the capacitance from the scavenging electrode to ground, C_t is the capacitance from the tuning electrode to ground, and C_{mut} is the capacitance between the scavenging and tuning electrodes. If the scavenging electrode is terminated with a simple resistor, the system can be described by equations 26 and 27.

$$m\ddot{z} + c\dot{z} + kz - \frac{dY}{t_p b_{1s}} V_s = -m\ddot{y} + \frac{dY}{t_p b_{1t}} V_t \tag{26}$$

$$C_p \dot{V}_s + \frac{1}{R_{load}} V_s = \frac{dAY}{b_{2s}} \dot{z} \tag{27}$$

where d is the piezoelectric strain coefficient, Y is Young's modulus, t_p is the thickness of the piezoelectric layer, b_{1s} is a constant that relates average stress under the scavenging electrode to a force at the end of the beam, b_{1t} relates stress under the tuning electrode to tip force, and b_{2s} relates average strain under the scavenging electrode to displacement of proof mass (z)[4].

We will assume that the tuning voltage is given by the relationship $V_t(t) = -aV_s(t)$, where a is just a constant gain factor. The power consumed by the tuning actuator is than just $P_t(t) = V_t(t)I_t(t) = -aV_s(t)I_t(t)$, the magnitude of which is given by $P = \frac{1}{2}C_t V_t^2 \omega = \frac{1}{2}a^2 C_t V_s^2 \omega$. For the purposes of this analysis, we will assume that no power is required to generate the signal for $V_t(t)$. In other words, no power is required to measure, invert, and amplify the signal from the scavenging electrode.

4. RESULTS

A prototype device, shown in Figure 8, was constructed, built and tested. The natural frequency of the device with the tuning electrode short circuited (ω_t) was measured as 67 Hz. A simple inverting amplifier circuit was used to invert and amplify the voltage signal from the scavenging electrode. This voltage was used to drive the tuning electrode.

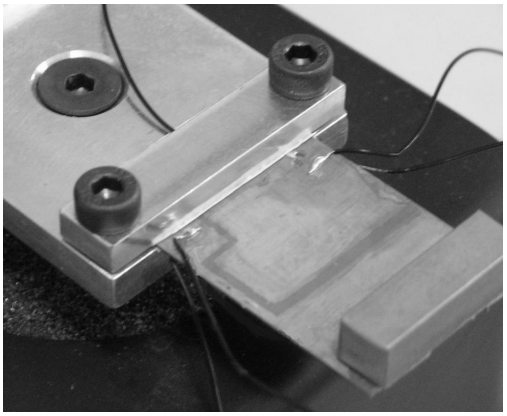

Figure 8. Photograph of generator with scavenging and tuning electrodes.

Using the dimensions and material properties of the prototype device, the system was simulated using equations 26 and 27 above. Figure 9 shows both the simulated and measured natural frequency versus the magnitude of the voltage placed on the tuning electrode ($|V_t|$). Five separate measurements of the relationship between the natural frequency and $|V_t|$ were performed and the results of all five measurements are shown in Figure 9. Figure 10 shows the simulated and measured actuation power versus the natural frequency.

Both Figure 9 and Figure 10 indicate that the simulation underestimates the voltage (and power) required for a given frequency change. Nevertheless, the shape of the simulated curves fits the measurement data, and the basic behavior is as expected.

Figure 11 shows the simulated powers versus frequency. $|P_{out1}|$ is the output power without tuning, $|P_{out2}|$ is the output power with tuning, $|P_a|$ is the actuation power, and $|P_{net}|$ is the net power change ($|P_{out2}| - |P_a| - |P_{out1}|$). Note that the actual situation is somewhat worse than indicated by Figure 11 because the measured actuation power for the same frequency change is greater than the simulated actuation power.

The scavenging electrode was terminated with a variable resistor and output power versus load resistance was measured for three cases:

1) device driven at the untuned natural frequency (67 Hz) with tuning electrode short circuited
2) device driven at tuned natural frequency (64.5 Hz) with tuning electrode short circuited
3) device driven at the tuned natural frequency (64.5 Hz) with tuning voltage of 5 volts in magnitude.

Power output versus load resistance for these three cases is shown in Figure 12. The actuation power for case 3 is 440 μW. Table 1 indicates the maximum power for each case, and the net power change from tuning.

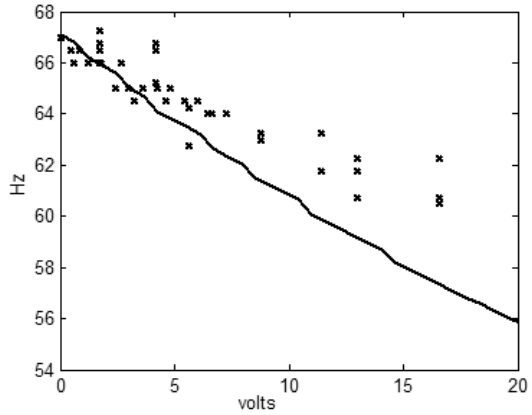

Figure 9. Simulated (line) and measured (crosses) natural frequency versus magnitude of the tuning voltage.

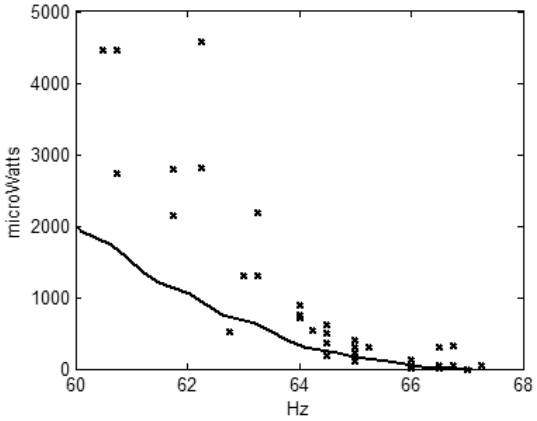

Figure 10. Simulated (line) and measured (crosses) actuation power versus natural frequency.

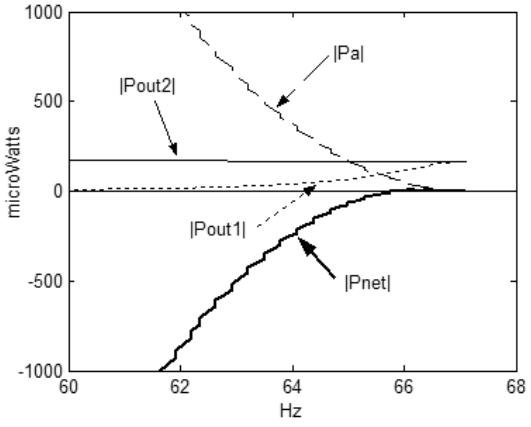

Figure 11. Simulated power output after tuning ($|P_{out2}|$), power output without tuning ($|P_{out1}|$), tuning actuation power ($|P_a|$) and net output power change from tuning ($|P_{net}|$) versus natural frequency.

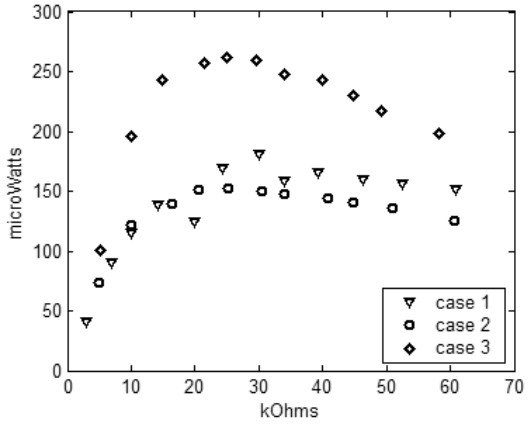

Figure 12. Measured power output from scavenging electrode vs. load resistance for three cases described above.

Table 1. Maximum power output (μW) for each of the three cases in Figure 12 and net power change ($|P_{net}|$) from tuning.

P (case 1)	P (case 2)	P (case 3)	$\|P_{net}\|$
180	152	262	-358

5. DISCUSSION OF RESULTS

The tunable generator shown in Figure 8 may not represent the most effective active tuning actuator. However, it does exhibit the basic intended behavior; the natural frequency changes in response to an input stimulus (a tuning voltage in this case) that must remain "active" as long as the tuned natural frequency is to be maintained. As predicted by the general linear transducer theory presented in section 2, the power required to tune the natural frequency far outweighs the increase in power output as a result of tuning.

The measured power output from the scavenging electrode while the tuning actuator is active (case 3 in Figure 12 and Table 1) is significantly larger than predicted by the mathematical model given in equations 26 and 27. Equations 26 and 27 predict that the power output for case 3 should be only 7 μW larger than that of case 1 instead of the 82 μW measured difference. The reason for this discrepancy is not entirely known. Equations 26 and 27 model the generator as a lumped parameter system, which may cause some error. More detailed modeling and further validating experiments are needed to identify the exact source of the discrepancy. However, the power output with the tuning actuator active is still well below the actuation power, and the net change in power output due to tuning is –358 μW. Therefore, while discrepancies between experiments and data exist, the experiments do validate the basic expected behavior.

More detailed modeling and further validating experiments may yield a better fit between experimental data and theory. However, as the experiments presented here do validate the basic conclusion that active tuning generators will not result in increased net power output, a more extensive round of tests would seem to be fruitless. The experimental data already supports the basic conclusion that "passive" tuning generators are the better of the two alternatives to frequency tuning of vibration based generators.

6. CONCLUSIONS

As the need for alternative power sources for wireless sensors becomes more acute, research on vibration based energy scavengers is becoming more prevalent. Almost all scavengers reported are resonant devices that rely on the natural frequency of the device being matched to the dominant frequency of the input vibrations. As most scavengers have quality factors of about 20, a scavenger that can tune its natural frequency to match that of the input vibrations could significantly broaden its application.

This paper has analyzed the feasibility of "active" tuning actuators. "Active" tuning actuators are distinguished from "passive" tuning actuators by their need for a constant power input to the tuning actuator while maintaining a tuned natural frequency. Using a standard, technology non-specific, model for vibration based generators[5] this paper has demonstrated that an "active" tuning actuator will never result in a net increase in power output. The power required to tune natural frequency will always exceed the increase in power output resulting from the frequency tuning.

A piezoelectric generator with an active tuning actuator has been built and tested. While there is some variability in the test data, and there is significant mismatch between theoretical calculations and experimental results, experiments validate the basic expected behavior. The change in power output (82 μW) as a result of tuning is significantly smaller than the power needed to drive the tuning actuator (440 μW).

As a result of this study, the authors believe that future research into frequency tuning of vibration based energy scavengers should focus on "passive" tuning actuators, which are able to cut power to tuning actuator while still maintaining the tuned natural frequency.

ACKNOWLEDGEMENTS

The authors would like to gratefully acknowledge Prof. Paul Wright, Eli Leland, V. Sundararajan, and the rest of the Berkeley Manufacturing Institute for many fruitful discussions on the topic of this paper.

REFERENCES

1. Hill J, Culler D (2002) Mica: A Wireless Platform for Deeply Embedded Networks. *IEEE Micro* 22(6):12-24
2. Glynne-Jones P, Beeby SP, James EP and White NM, (2001) The modelling of a piezoelectric vibration powered generator for microsystems. *Transducers 01 / Eurosensors XV*, June 10 – 14, 2001.
3. Ottman GK, Hofmann HF, Lesieutre GA (2003) Optimized piezoelectric energy harvesting circuit using step-down converter in discontinuous conduction mode. *IEEE Transactions on Power Electronics*, 18(2), 696-703.
4. Roundy S, Wright PK, Rabaey J (2003) *Energy Scavenging for Wireless Sensor Networks with Special Focus on Vibrations*, Kluwer Academic Press, ISBN Number 1- 4020-7663-0.
5. Williams CB, Yates RB, (1995) Analysis of a micro-electric generator for Microsystems. *Transducers 95/Eurosensors IX*, 1995, 369 – 372.
6. Amirtharajah R, Chandrakasan AP (1998) Self-Powered Signal Processing Using Vibration-Based Power Generation. *IEEE Journal of Solid State Circuits*, 33(5), 687-695.
7. El-hami M, Glynne-Jones P, White NM, Hill M, Beeby S, James E, Brown AD, Ross JN (2001) Design and fabrication of a new vibration-based electromechanical power generator. *Sensors and Actuators, A: Physica*l, 92(1-3):335-342.
8. Meninger S, Mur-Miranda JO, Amirtharajah R, Chandrakasan AP, Lang JH, (2001) Vibration-to-Electric Energy Conversion. *IEEE Trans. VLSI Syst*., 9 : 64-76.
9. Roundy S, Wright PK, Pister KSJ (2002) Micro-Electrostatic Vibration-to-Electricity Converters, *ASME IMECE*, Nov. 17-22, 2002, New Orleans, Louisiana.
10. Miyazaki M, Tanaka H, Ono G, Nagano T, Ohkubo N, Kawahara T, Yano K (2003) Electric Energy Generation Using Variable-Capacitive Resonator for Power-Free LSI: Efficiency Analysis and Fundamental Experiment. *ISPLED 2003*, August 25-27, 2003, Seoul Korea.
11. Adams SG, Bertsch FM, Shaw KA, Hartwell PG, Moon FC, and MacDonald NC (1998) Capacitance based tunable resonators. *J. Micromech. Microeng*. 8: 15-23.